# EXPERIMENTAL VERIFICATION OF SIMULATED PREDICTIONS FROM THE DDSI INSTRUMENT

**Sophie Grape**
Uppsala University

**Erik Branger**
Uppsala University

**Zsolt Elter**
Uppsala University

## ABSTRACT

The Differential Die-away Self Interrogation (DDSI) instrument was researched for many years under the Next Generation Safeguards Initiative Spent Fuel effort. Later a prototype instrument was manufactured and used to make non-destructive measurements of spent nuclear fuel in the Swedish Central Interim Storage Facility for Spent Nuclear Fuel (Clab) in Sweden in 2018. Results of DDSI research, based on either simulations or measurement time, have indicated that the instrument could successfully be used to draw safeguards-relevant conclusions about spent nuclear fuel.

In this work we investigate how well the modelled response of the DDSI instrument, based on Serpent and MCNP simulations, corresponds to measured data of 17x17 pressurised reactor fuel. We also studied repeatability, i.e. to what extent repeated measurements on the same fuel assembly gave consistent results. We also investigated the dependence of tau on the selected time window. The results show that tau values determined from measurement data are consistently higher than tau values determined from simulations, and that the magnitude of tau is dependent on the choice of time window. We also note that tau is relatively insensitive to positioning in the DDSI instrument.

**Keywords**: DDSI, neutron measurements, spent fuel verification, safeguards

## 1. INTRODUCTION

Research is ongoing to develop new non-destructive assay (NDA) instruments and analysis techniques that can quickly and reliably assess properties of spent nuclear fuel. The aim is to support the nuclear safeguards inspectors with more accurate, effective and efficient tools that help draw conclusions on whether or not declarations from States are complete and correct.

The DDSI measurement technique was further developed to assay spent nuclear fuel and their properties under the US DOE NNSA's Next Generation Safeguards Initiative Spent Fuel (NGSI-SF) project [1]. The measurement technique is sensitive to the amount of fissile material in the fuel assemblies, and was first thoroughly investigated using simulations before a prototype instrument was built and tested on both fresh and spent nuclear fuel [2, 3]. The measurements on spent nuclear fuels were performed in 2018 and included 25 PWR and 25 BWR spent fuel (SF) assemblies with diverse attributes at the Central Spent Fuel Interim Storage Facility (Clab) in Sweden. Despite a failure of two of the four detector pods, the subsequent analysis showed that multiplication, fissile mass, initial enrichment, burnup, and total plutonium mass could indeed be successfully determined using the data [3].

In this work, we investigate the level of agreement between predictions of the early die-away time (known as tau) using Serpent and MCNP6 and the experimentally measured tau values

using different fitting ranges, from here on referred to as time windows. This allows for a direct comparison of predicted and measured tau values. An evaluation of uncertainties in tau due to the positioning of the fuel assembly (FA) inside the instrument is also included.

## 2. THE DDSI PRINCIPLE

The DDSI principle is exhaustively described in [4]. It is a passive NDA technique, relying on neutron coincidence counting, developed to assay nuclear material such as spent nuclear fuel (SNF). In SNF, the presence of radionuclides such as 244Cm that undergo spontaneous fission, act as a source of neutrons which interrogate the fissile content of the fuel. The neutrons emitted in spontaneous fission are moderated in the water, before inducing new fission in primarily 235U, 239Pu, and 241Pu. Depending on the multiplication (related to the composition of the spent nuclear fuel), fission chains with various lengths will develop. By recording neutrons in list-mode, knowledge about the neutron population and its evolution over time can be obtained.

The early die-away time tau quantifies the neutron population lifetime inside the SNF. It can be determined using a fit to a neutron coincidence time distribution known as the Rossi-Alpha Distribution (here referred to as RAD) in the approximate time window of 4-52 mus [5]. The RAD describes the number of neutrons detected in coincidence with any first neutron as a function of time, and each time bin corresponds to a specific time gate with respect to the first neutron. The RAD can be described (also in this work) by a single exponential function in a limited time span, although the underlying physics processes originate from two different sources (each of which can be described by an exponential function) [4]. One process concerns time-correlated neutrons coming from the same fission chain, or fast fission processes. The second process concerns time-correlated neutrons coming from fission reactions in the same fission chain, where at least one following fission was induced by a thermal neutron. The so-called early die-away time, tau, can be determined in a specific time range of the RAD, where both components are present, and therefore properties of the SNF (such as abundance of fissile and neutron absorbing material) as well as properties of the DDSI instrument (instrument design), play a role. Previous simulation work [5] has indicated that in the time window of 4-52 mus, the early die-away time is quadratically related to the multiplication of the SNF, and this is what makes the signal relevant in the context of SNF verification for nuclear safeguards purposes.

## 3. SF MEASUREMENTS AT CLAB

During a measurement campaign in 2018 at Clab in Sweden, the DDSI prototype instrument was tested in the field on SNF. During the campaign, both BWR fuels and PWR fuels were measured, but unfortunately only two of the detector pods proved to be operational and collected data. The instrument is shown in Figure 1.

In this work we focus on measurements of the 17x17 PWR fuels. These SNFs have an IE in the range of 2.1-3.9%, a BU of 20-47 MWd/kgU and a CT of 10- 32 years. Reference [3] summarises the measurement campaign, the DDSI instrument as well as the results from the measurements on prediction capabilities of fuel properties.

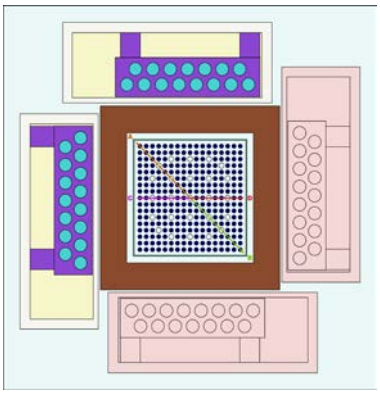

**Figure 1. The DDSI prototype instrument. Arrows denote fuel movements inside the instrument, investigated later in this work.**

# 4. MODELLING SNF AND THE DDSI INSTRUMENT RESPONSE

The DDSI instrument and its measured response to the 17x17 fuel assemblies has been investigated before [3]. Ref [6] described the details of the SF modelling performed using the three-dimensional depletion code ORIGEN Assembly Isotopics (ORIGAMI) to estimate the predicted response including FA multiplication. In this work, we have used the Monte Carlo code Serpent2 [7] for depletion calculations, and MCNP6 [8] for particle transport and detection in the DDSI instrument. Comparing the simulations in this work to those in [6], we note that reference [6] provides a much more detailed model by including pin-by-pin burnups and axial burnup profiles, and that it also considers control rod insertion histories in order to generate nuclide compositions in specified fuel pin segments. However, the level of details included in the Serpent and MCNP simulations performed here reflect the level of details an inspector could expect to receive in connection to routine safeguards inspections (ie. data on IE, BU and CT but not detailed fuel irradiation information).

## 4.1 Fuel modelling and burnup calculations in Serpent

An infinite 2D lattice in criticality source mode was implemented in Serpent2 in order to perform fuel burnup calculations and estimate the material composition of the SNF. The fuel rods were defined with a radius of 0.41 cm and a 0.01 cm gap to the cladding which has an outer radius of 0.48 cm. The pitch between fuel rods was 1.26 cm. These dimensions correspond to a generic PWR17x17 assembly, and are judged to be representative of the measured PWR assemblies. A default irradiation scheme of 365 days of irradiation was assumed, followed by 30 days of downtime, resulting in a default burnup of 10 GWd/tU per full cycle. The duration of the last cycle was adjusted to result in the desired discharge BU value, as provided by the operator for each FA. The BU step was 0.5 GWd/tU.

## 4.2 DDSI instrument response calculations using MCNP

The DDSI prototype instrument submerged in water was implemented in MCNP6 following the description in [4]. The fuel pin geometry was the same as in the Serpent calculation, but implemented in a 17x17 FA design. All fuel pins had the same material composition, taken from the output of the Serpent2 calculations. A spontaneous fission source was evenly distributed across all fuel pins, but restricted in axial direction to 145 cm centred on the DDSI prototype instrument, because assessments showed that regions farther from the instrument did not contribute to the detector signal. Detailed specifications on the instrument geometry can be found in [4]. The neutron detection was simulated with F8 capture tallies in the 3He tubes (having an active length of 40 cm). One hundred F8 tallies, each with 2 μs gates, were

used to create the RAD of true neutron coincidences. As only two (adjacent) of the four pods were operational during the experimental measurement campaign at Clab, only two detector pods were simulated to be functioning (and contributing to the tallies) MCNP6, and the other two were kept in the MCNP6 model, but were considered to be filled with water.

# 5. ANALYSIS

## 5.1 The RAD

During the measurements at Clab, the National Instruments List-Mode Acquisition (NILA) software on the data acquisition system was used to record neutron timing information. In a second step, a custom version of the FastTapX software, referred to as FastTapX-DDSI [9], was used to produce RADs. The RADs describe detected neutrons in a specific time gate as a function of time. Although the modelled RADs do not contain any accidentally detected neutrons in coincidence with unrelated fission events or experimental effects such as deadtime or pile-up in the detectors, the measured RADs do and need to be corrected for that. A characteristic fall-off behaviour of the RAD can be observed, determined by the relative fraction of detected neutrons coming from the same fission event as the initially detected neutron, or from two different fission events in the same chain. For most fuels, the RAD is recorded up to 1000 mus, and the rate of accidental coincidences can be estimated and subtracted using a constant fit in the range of 400 mus<t<1000 mus where only accidental coincidences occur. After subtraction of the accidental neutrons, an exponential fit was made to determine the early die-away time tau from the RAD.

Figure 2 shows one example of a simulated RAD shown together with an experimentally measured RAD after background subtraction, for one particular FA. The same figure shows exponential fits to the data, using the suggested time window of 4-52 mus. It can be noted that the amplitude of the experimental RADs is substantially lower than in the simulations, and the experimental RAD shows a “peak” at short times (meaning that fitting an exponential curve to the RAD before the peak will introduce errors). This position of the peak is different for each fuel assembly and it varies with up to six microseconds. It can also be seen that the experimentally measured RAD is initially rising, and that the expected fall-off behaviour sets in at around 10 mus. The reason for the “peak” is that the He3 detectors suffer from dead time and pulse pileup, which prevents the exponential behaviour seen at longer time to continue all the way down to time zero. To ensure that the loss of events in this region does not bias the measurements, coincidence counting should be avoided until the fall-off behaviour has set in.

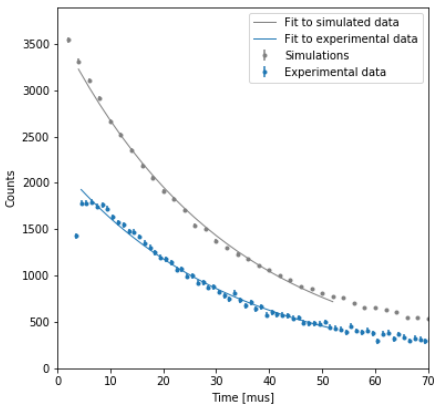


**Figure 2. Example of a simulated RAD (grey) and a measured, background-subtracted, RAD (blue) together with exponential fits.**

5.2 Tau analysis

In reference [3], the time window used to determine tau from experimental data was different from the one used in the simulations (4-52 mus). The reason was the "peak" feature of the experimental RADs, which did not enable an exponential fit to start already at 4 mus. Instead, a 57 mus long time window starting from 13-70 mus was selected, because this starting point would be above the "peak" for all fuel assemblies. In [3], it was found that the tau values from the measurements were proportional to multiplication, but whether they agreed with the predictions from the simulations or not was outside the scope of the work.

*5.2.1 Investigating dependence on M*

In this work, we have analysed the use of different time windows to determine tau, keeping in mind that its relationship to M must not be affected. Initially, the analysis in [3] was repeated. The results of the determination of tau using the same measurement data, reveals that we can confirm the proportionality between tau and multiplication, shown in Figure 3. The figure shows tau, determined in the range of 13-70 mus, plotted against net multiplication (M) determined in the MCNP simulations. Fuel assemblies measured multiple times are shown with different markers. One can observe two clusters of data in the figure. In the left cluster, the tau values are plotted against M-values from [3], and in the right cluster tau plotted against M determined in this work. It can be seen that the M-values vary considerably, despite the fact that they were both determined using MCNP (however the underlying depletion calculations differed). One can also note that the range of M-values is different for the two clusters. The span is about 0.35 for the ORIGAMI/MCNP simulations, and around 0.55 for Serpent2/MCNP simulations. The modelling of the fuel assemblies in [3] was done according to the description in [10] and using the 3-dimensional ORIGAMI code which considers detailed operator-provided information such as pin-by-bin burnups, axial burnup profiled, in-core measurement data and full reactor operating records. The SOURCES code was then used to generate neutron source terms for each fuel pin from the resulting isotopic compositions. In this work, the depletion calculations were done in Serpent using a fuel-pin model and assuming that all fuel rods in an assembly are identical. Only information on average power and burnup-per-cycle was considered, as more detailed information is typically not available to safeguards inspectors.

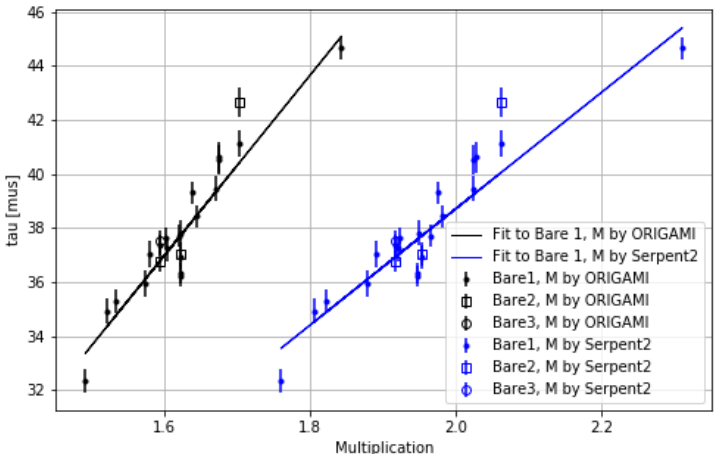


**Figure 3. Tau determined using the time window 13-70 mus versus M from [3] (left or black cluster) and M from Serpent 2 (right or blue cluster), together with fits. Bare1= first measurement of each FA, "Bare2"= second measurement, and "Bare3" third measurement.**

Figure 3 shows that two SNF were measured repeatedly; one was measured twice with statistically different tau values and the other was measured three times and using this particular time window two of the tau values were consistent with each other. Differences in tau upon measuring the same FA under the same conditions could be due to positioning of the assembly inside the DDSI instrument (as pointed out in reference [11]). This is not anticipated to play a role with four functioning detector pods since the assembly being further away from one pod means that it is closer to the opposite pod, thus cancelling the effect. However for a non-symmetrical 2-pod case, such effects are not cancelled.

*5.2.2 Comparing measurements with simulations for different time windows*
Figure 4 shows the experimentally determined tau values, determined in the time window of 13-70 mus, versus simulated tau values, determined in the time window of 4-52 mus. Ideally these would agree perfectly with data points positioned on the orange line.

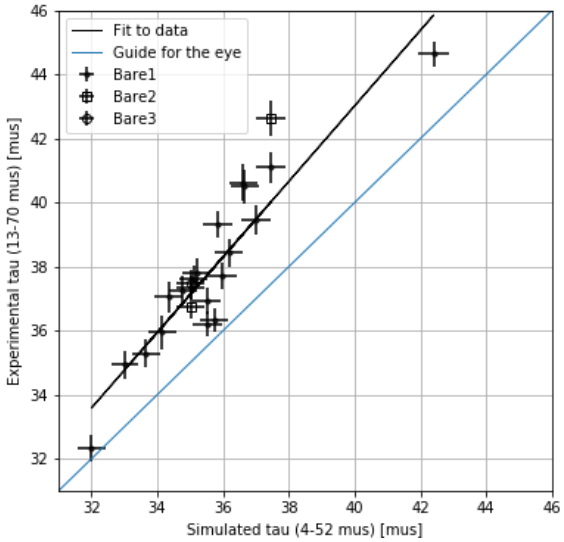


**Figure 4. Experimentally determined tau versus simulated tau, with a fit to data (black line) and a guide for the eye (blue line).**

Figure 4 shows that the tau values from experimental data are systematically higher than those from simulations. The fact that the tau values do not agree is however not surprising, since the tau values are determined using different time windows. Thinking back on the RAD, we know that it can be explained by neutrons with different origins (the fast and slow component), and that the contribution to the RAD by each component varies with time. Thus, tau values determined with different time windows could describe different fractions of the fast and slow component, and thus (to a limited extent) describe different physics.

Although it is not possible to use the proposed time window of 4-52 mus in the analysis of experimental data (since many RADs are still rising at that point), it is possible to investigate if any other time window would result in a better agreement between simulated and experimentally determined tau values. In order for tau to be a useful parameter, it should be related to multiplication (reference [5] reports that the early die-away time from the DDSI instruments response is quadratically related with the SFA multiplication). In addition, tau should be stable enough to allow for repeated measurements to yield similar estimates of tau. One naïve option when analysing measurement data is to start the fit at the maximum RAD amplitude and to end the time window at 52 mus. This would make the time window somewhat shorter, but it would maximise the use of the suggested time window. That was

tested in this work, but proved not to be a good choice, because the maximum RAD is not always a clearly defined point in time, but looks more like a (small) plateau. This means that the exponential fall-off behaviour does not set in immediately after the maximum RAD has been reached, and an exponential fit starting at that time does not well describe the data. Another example would be to start the fit slightly later (for instance 3 mus later), to avoid starting the fit too early. A third option could, for instance, be to use a longer time window, matching the range used in analysis of the measurement data. Tau results of these different approaches will be shown in this work.

Figure 5 shows the experimentally determined tau values plotted against the simulated tau values, in order to see how well they agree. Different time windows are used to determine the tau values. The figure shows that there is a slight offset in both subfigures, and the offset depends on the choice of time window. One can also note that the slope of the fits slightly varies, but is close to 1. With a longer time window, the absolute values of tau increase and the uncertainties in tau due to the fit become smaller.

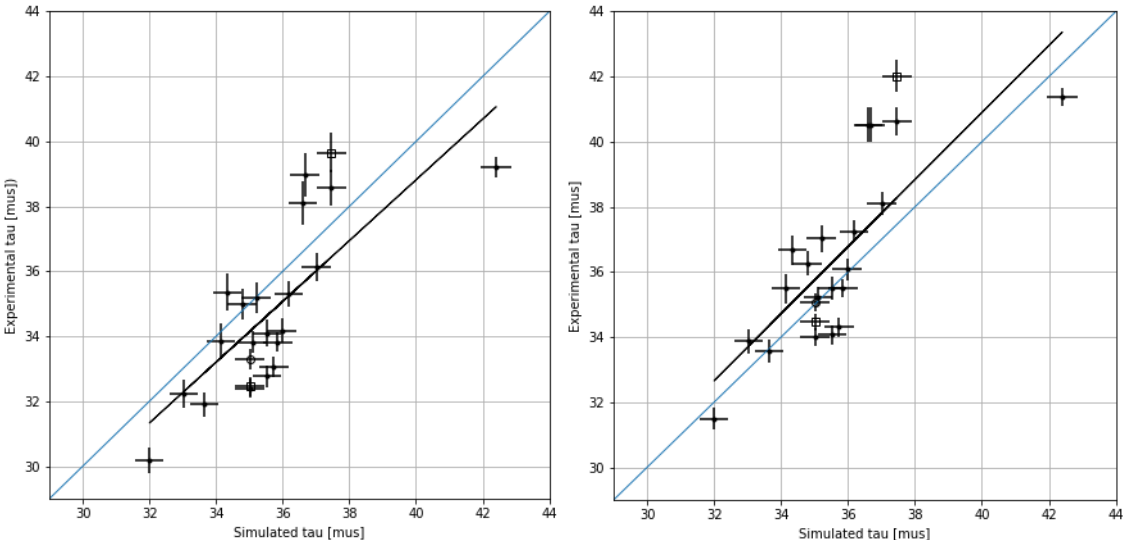


**Figure 5. Experimentally determined tau values versus simulated tau. Left panel: time window starts 3 mus after the maximum RAD and lasts until 52 mus. Right panel: time window starts 3 mus after the maximum RAD and lasts for 57 mus (to match the longer time window range of 13-70 mus).**

Of key importance in this context is the proportionality between tau and multiplication, since that is what makes tau interesting to study from a safeguards point-of-view. Figure 6 shows tau values determined from measurements, obtained using different fit windows, plotted against M. The two time windows used in the analysis of data shown in Figure 6 are included here to represent examples of a much larger number of cases investigated in this project; all of which showed similar features. We observe that the values of tau changes depending on the length of the time window. The shortest fit window results in the lowest tau values, and the longest time window results in the largest tau values.

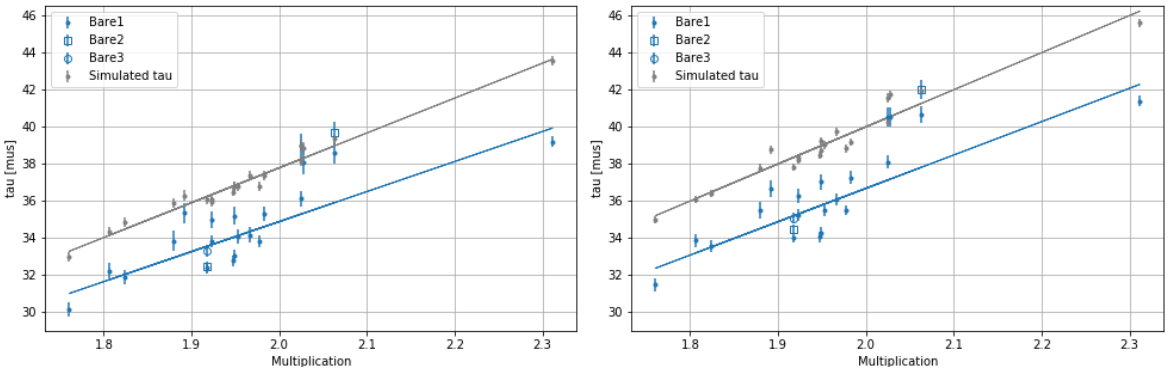


**Figure 6. Simulated and experimentally determined tau values versus multiplication. Left panel: time window starts 3 mus after the maximum RAD and lasts until 52 mus. Right panel: time window starts 3 mus after the maximum RAD and lasts for 57 mus (to match the longer time window range of 13-70 mus).**

The results of the tau analysis show that the choice of time window affects both the absolute value of tau (with tau changes on the 5-10% level) and the uncertainty in its determination (based on the statistics in the RAD). The trend is that longer time windows correspond to larger tau values and lower uncertainties. We also note that whether or not repeated measurements are found to result in significantly different tau values or not depend on, among other things, the time window used in the determination of tau. Other causes may potentially be related to the positioning of the FA in the DDSI instrument, and will be investigated later in this work.

From the results in Figure 6 it is not obvious that one time window is superior to another. Clearly, different time windows can be used to determine tau values that are proportional to multiplication and no matter what time window that is selected, some offset remains between simulated tau values and tau values determined from measurement data. In order to assess if the simplified fuel irradiation history was the cause of the difference between the simulated and measured results, simulations were run using the detailed irradiation history. The results showed that the impact of this was minimal, and is not be the reason for the discrepancy between tau values determined from simulations and experimental data. What we can conclude at this stage is that with respect to the fit, it is important to not start it until the fall-off behaviour of the RAD has set in, and that to use the same time window throughout the analysis of simulated and measured data if the analyst is interested in relating the tau values to each other on more than a relative scale.

## 5.3 EFFECT ON TAU OF FUEL POSITIONING

As mentioned earlier, two fuel assemblies were measured multiple times; one of them twice and the other one three times. The results presented in Figures 5 and 6 show that the determined tau values are not agreeing with each other, if only uncertainties from the fit are considered. In this work, we are investigating whether the positioning of the fuel in the DDSI instrument could cause the disagreement of the tau values.

The central part of the DDSI instrument consists of a funnel which safely guides the FA into position. The positioning procedure does however not ensure that the fuel is exactly in the center of the instrument, or that there is equally much water on all sides of the FA. If all four detector pods are working it will not matter if the assembly is centred or not. However, if two detector pods malfunction, the positioning becomes more important because of the non-symmetrical configuration. In order to allow for some wiggle room, the inner distance

between the funnel walls is 22.2 cm apart, and the width of the PWR FA is 21.42 cm. This leaves 0.39 cm of water on every side of the FA, if it is centred inside the DDSI instrument. In addition, there is a distance between the spacers that hold the fuel rods together (marking the FA edge), and the outer edge of the outermost fuel rod; this distance is 0.15 cm. If the DDSI instrument is positioned around the FA where there are no spacers, it is (at least in theory) possible to have a water gap of 0 cm on one side, and of 2x(0.39+0.15)=1.08 cm on the opposite side. This estimate does not consider the possible movement of the detector pods, which are firmly attached at the top but not at the bottom (they could in principle have a small angle relative to the FA, with the largest water gap at the bottom being less than 5 mm according to [4]).

Simulations were performed for a fuel positioned in the centre of the funnel, and in four other positions. Considering that the two functioning detector pods were placed adjacent to each other we decided to place fuel FA i) as close as possible to both functioning detector pods (Position A) ii) as far away as possible from both detector pods (Position B), iii) as close as possible to one detector pods and centrally placed with respect to the other (Position C), and iv) as far away as possible from one detector and centrally placed with respect to the other (Position D). The movements are indicated in Figure 1.

From the simulations, the tau was determined again according to the same methodology as described earlier and using the time window from 4 to 52 mus. The different tau values are shown in Table 1.

**Table 1. The tau values for the different fuel positions inside the DDSI instrument.**

| FA position | Tau [mus] |
|---|---|
| Default (centrally positioned) | 39.80 ± 0.45 |
| Position A (SFA  moved up and to the left) | 39.10 ± 0.42 |
| Position B (SFA moved down and to the right) | 40.76 ± 0.48 |
| Position C (SFA moved to the left) | 38.79 ± 0.43 |
| Position D (SFA moved to the right) | 39.94 ± 0.46 |

As can be seen in Table 1, the tau value from the centrally placed FA agrees within uncertainties with tau values calculated from three of the four investigated positions. The shortest tau values obtained with the FA as close as possible to one detector pod and centrally placed with respect to the other one. One can above all note that the difference in tau as a function of the positioning cannot fully account for the deviations in tau values observed when measuring the same FA multiple times (which is on the order of 2 mus for one fuel assembly).

# 6. SUMMARY AND CONCLUSION

The DDSI measurement technique offers a way to non-destructively assess the fissile material in spent nuclear fuel assemblies. It does so by quantifying the die-away time tau of the neutron population in a spent nuclear FA. In this work, we have re-analyzed DDSI measurement data from SNF at Clab, with the objective of evaluating the level of agreement of tau determined from simulated and measured data. The results show that the measurements result in larger tau values than the simulations, and that this difference persists even when using other time windows to determine tau. We also note that the choice of time window in the analysis impacts the value of tau. The effect on tau of positioning the SFA inside the DDSI instrument was also studied and the results indicate that this impact is low and cannot

account for the difference in tau values observed when analysing data of repeated measurements.

# 7. ACKNOWLEDGEMENT

We would like to acknowledge Li Pöder Balkeståhl for her contributions to the developments of the scripts used in this analysis, and thank Alexis Trahan and Holly Trellue for their interest in this work and all DDSI discussions. This work was performed with support of the Swedish radiation safety authority under contract SSM2022-1105.

# 8. REFERENCES

[1] S. Tobin, et al., "Experimental and Analytical Plans for the Nondestructive Assay System of the Swedish Encapsulation and Repository Facilities," in IAEA Symposium, IAEA-CN-220-238 (2014)
[2] A. C. Trahan, A. P. Belian, M. T. Swinhoe, H. O. Menlove, M. Flaska and S. A. Pozzi, Fresh Fuel Measurements With the Differential Die-Away Self-Interrogation Instrument, in IEEE Transactions on Nuclear Science, vol. 64, no. 7, pp. 1664-1669 (July 2017)
[3] Alexis C. Trahan, Garrett E. McMath, Paul M. Mendoza, Holly R. Trellue, Ulrika Backstrom, Li Pöder Balkeståhl, Sophie Grape, Vlad Henzl, Daniel Leyba, Margaret A. Root, Anders Sjoland, Results of the Swedish spent fuel measurement field trials with the Differential Die-Away Self-Interrogation Instrument, Nuclear Instruments and Methods in Physics Research Section A: Accelerators, Spectrometers, Detectors and Associated Equipment, Volume 955 (1 March 2020)
[4] Alexis Chanel Trahan, Utilization of the Differential Die-Away Self-Interrogation Technique for Characterization and Verification of Spent Nuclear Fuel, Doctoral thesis, University of Michigan (2016)
[5] A. C. Kaplan, V. Henzl, A. P. Belian, H. O. Menlove, M. T. Swinhoe, M. Flaska, S. A. Pozzi, Determination of Spent Nuclear Fuel Assembly Multiplication with the Differential Die-Away Self-Interrogation Instrument, Nuclear Instruments and Methods A, Vol. 757, No.1 (2014).
[6] Jianwei Hu, Ian C. Gauld, Vladimir Mozin, Stephen Tobin, Stefano Vaccaro, Martin Bengtsson, Anders Sjöland, and Andrew Worrall, High-Fidelity modeling of spent fuel assemblies for advanced NDA instrument testings, Advances in Nuclear Proliferation Technology & Policy Conference, Santa Fe, New Mexico, United States of America, Sep 25, 2016 - Sep 30 (2016)
[7] Jaako Leppänen et al., The Serpent Monte Carlo code: Status, development and applications in 2013, Annals of Nuclear Energy, 82, pp. 142-150 (2015).
[8] MCNP6 user's manual version 1.0 edited by D. Pelowitz, LA-CP-13-00634 2013
[9] Henzl, K. Koehler, C.O. McGahee, FastTap and fastTrain: How to create neutron multiplicity pulse train data when you are not an experimentalist, in: INMM 57th Annual Meeting, Atlanta, GA (2016).
[10] Jianwei Hu, Ian C. Gauld, Vladimir Mozin, Stephen Tobin, Stefano Vaccaro, Martin Bengtsson, Anders Sjöland, and Andrew Worrall, High fidelity modeling of spent fuel assemblies for advanced NDA instrument testings
[11] A. Trahan, G. E. McMath, P. Mendoza, H. Trellue, U. Backstrom, A. Sjoland, Preliminary Results from the Spent Nuclear Fuel Assembly Field Trials with the Differential Die-Away Self-Interrogation Instrument, 59th Annual Meeting of the Institute of Nuclear Materials Management (INMM 2018)